

Disorder Effect on the Vortex Pinning by the Cooling-Process Control in the Organic Superconductor κ -(BEDT-TTF)₂Cu[N(CN)₂]Br

N. Yoneyama, T. Sasaki, N. Nishizaki, and N. Kobayashi

Institute for Materials Research, Tohoku University, Sendai 980-8577, Japan

(Dated: October 28, 2018)

We investigate the influence of disorders in terminal ethylene groups of BEDT-TTF molecules (ethylene-disorders) on the vortex pinning of the organic superconductor κ -(BEDT-TTF)₂Cu[N(CN)₂]Br. Magnetization measurements are performed under different cooling-processes. The second peak in the magnetization hysteresis curve is observed for all samples studied, and the hysteresis width of the magnetization becomes narrower by cooling faster. In contradiction to the simple pinning effect of disorder, this result shows the suppression of the vortex pinning force by introducing more ethylene-disorders. The ethylene-disorder domain model is proposed for explaining the observed result. In the case of the system containing a moderate number of the ethylene-disorders, the disordered molecules form a domain structure and it works as an effective pinning site. On the contrary, an excess number of the ethylene-disorders may weaken the effect of the domain structure, which results in the less effective pinning force on the vortices.

I. INTRODUCTION

BEDT-TTF based organic superconductors, where BEDT-TTF is bis(ethylenedithio)tetrathiafulvalene, have the layered structure and the two-dimensional electronic properties.¹ As a feature of molecular-based compounds, the internal degree of freedom in the BEDT-TTF molecule can give a positional disorder.

The terminal ethylene groups of the molecule can be thermally excited between two conformations, “eclipsed” and “staggered” (Fig. 1). In the present compound, κ -(BEDT-TTF)₂Cu[N(CN)₂]Br, one of the ethylene group in a molecule is known to be disordered and the other ordered at room temperature,² where the eclipsed conformation is stable. Such a thermal excitation is observed in the narrowing effect of the ¹³C-NMR line width above ~ 150 K.³ The conformational disorder (ethylene-disorder) is frozen by quenching, and the introduction of the ethylene-disorders slightly affect the electronic state. The resistivity below about 80 K depends on cooling-rate,⁴ and in addition the superconducting transition temperature T_c is also reduced by cooling faster.⁵ The heat capacity measurement suggested that a glass tran-

sition is caused by freezing of the motion in the ethylene group around 100 K.⁶ Tanatar *et al.* proposed the T - P phase diagram on ordering of the ethylene groups.⁷ Stalcup *et al.* reported that a time-dependent resistivity is correlated with T_c and the amplitude of the Shubnikov-de Haas oscillation in terms of the ethylene-disorders.⁸ However, none of the reports have clarified the spatial distribution of the ethylene-disorders at all.

On the superconducting mixed states of the κ -phase BEDT-TTF organic superconductors, following features have been observed; the wide reversible magnetization regime,⁹ the second magnetization peaks,^{10,11,12,13,14} and the first-order phase transition between the vortex solid and liquid states.^{15,16,17,18} Taniguchi and Kanoda reported the cooling-rate dependence of the magnetization curves,¹² where the hysteretic magnetization width becomes narrow by cooling fast. One may consider that cooling fast introduces a much larger number of the ethylene-disorders, and leads to much stronger vortex pinning on the basis of a concept of the simple pinning effect by disorder. Nevertheless, this expectation does not agree with their experiments. The nature of this controversial result is unclear.

In this paper, we report detailed measurements of the hysteretic magnetizations under the control of cooling-process. We clarify the effect of the ethylene-disorders on the vortex pinning, and discuss the spatial distribution of the ethylene-disorders for explaining the observed results. We propose that domain structures originated from the ethylene-disorders work as a pinning site.

II. EXPERIMENTALS

Single crystals were synthesized by means of electrocrystallization. All the measurements of the magnetization were performed using a SQUID magnetometer (Quantum Design, MPMS-5) for a single crystal with the dimension of $1.8 \times 1.6 \times 0.3$ mm³. No grease was used to avoid strain to the sample. The magnetic-field

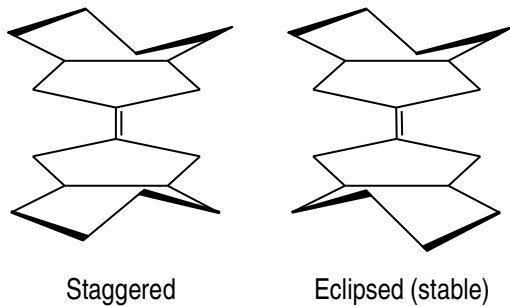


FIG. 1: Schematic view of conformational disorder in BEDT-TTF.

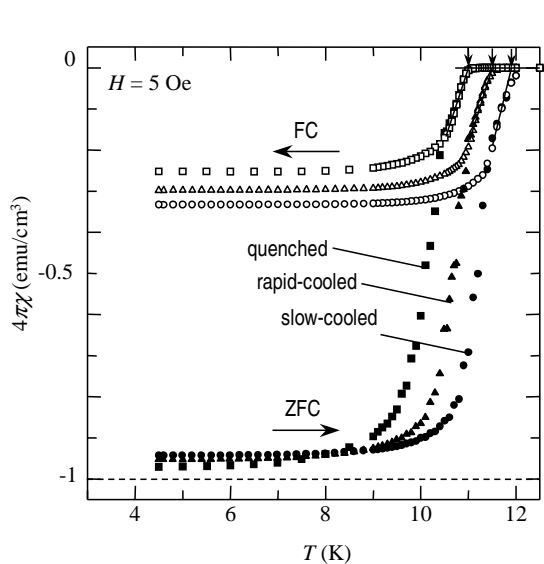


FIG. 2: Temperature dependence of the static magnetic susceptibility at 5 Oe. The closed and open symbols indicate the shielding curve measured under a zero-field-cooling condition (ZFC) and the Meissner curve under a field-cooling (FC), respectively, with overlaid for the slow-cooled (circles), rapid-cooled (triangles), and quenched processes (squares). The broken line shows the full-Meissner volume.

was applied perpendicular to the conduction plane. The cooling-process was controlled from room temperature to 15 K as follows; (1) 0.17 K/min with 30 h anneal at 70 K (slow-cooled), (2) 15 K/min (rapid-cooled), and (3) 100 K/min (quenched). After all the sequential measurements of the quenched sample, the data taken in the slow-cooled process again were completely reproduced, suggesting no deterioration of the sample by quenching, such as micro cracks. We carried out the similar measurements for other two samples, which indicate the same results with the present report.

III. RESULTS

Figure 2 shows the temperature dependence of the static magnetic susceptibility at 5 Oe. After subtracting the contribution of the core diamagnetization (-4.8×10^{-4} emu/mol), the demagnetization factor was corrected using an ellipsoidal approximation. T_c 's defined as an intercept of the extrapolated lines of the normal and reversible susceptibilities are 11.9, 11.5, and 11.0 K in the slow-cooled, rapid-cooled, and quenched process, respectively (short arrows in Fig. 2). The suppression of T_c by cooling faster is quantitatively consistent with the previous report.^{5,19} The magnetizations under a zero-field-cooled (ZFC) condition (shielding curves) show almost the full Meissner volume and the negligible cooling-rate dependence within the accuracy of our measurement. This result demonstrates that the superconducting

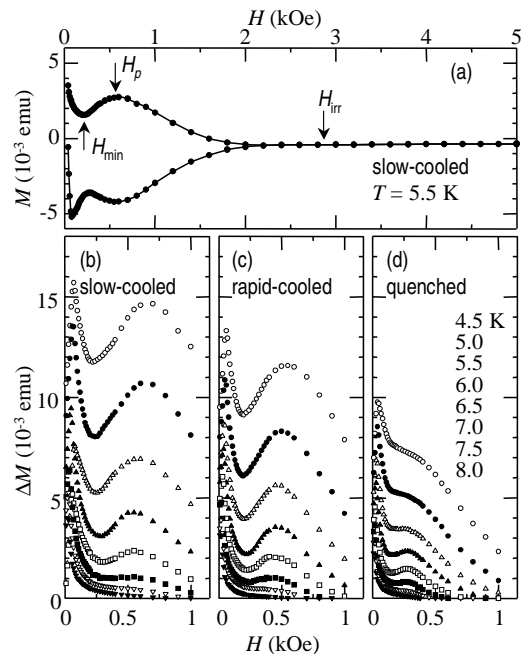


FIG. 3: Magnetic-field dependence of (a) the magnetization at 5.5 K, and the magnetization hysteresis width for cooling-rates of (b) slow-cooled, (c) rapid-cooled, and (d) quenched condition, respectively.

volume fraction is almost unchanged by cooling-process, whereas Pinterić *et al.* reported a small suppression of the superconducting volume fraction by faster-cooling.¹⁹ On the other hand, the magnetic susceptibilities under a field-cooled (FC) condition (Meissner curves) are reduced in comparison with those under the ZFC condition (open symbols in Fig. 2). The volume fractions are slightly suppressed with increasing cooling-rate. At first sight, the suppression might be attributed as reinforcement of vortex pinning by cooling fast, because smaller exclusion of magnetic-field generally reflects stronger pinning. However, as shown later, the experimental results in higher magnetic-fields are inconsistent with this explanation. We so suggest the other scenario as follows. It should be noted that the magnetic-field of 5 Oe for the susceptibility measurements is not sufficiently smaller than $H_{c1}(0) = 19$ G.²⁰ $H_{c1}(0)$ seems to decrease with T_c by cooling faster, and therefore the effective field $H/H_{c1}(0)$ is increased. This makes the flux exclusion more incomplete, leading to the further suppression of the FC superconducting volume by cooling faster.

Figure 3(a) shows the magnetic-field dependence of the magnetization at 5.5 K. A typical second peak is found around 500 Oe. As displayed in the magnetization hysteresis width ΔM (Fig. 3(b)–(d)), the second peak is observed below about 8 K for all the cooling-process. The peak height seems to decrease with increasing cooling-rate as reported previously.¹² Strictly speaking, to depict the cooling-rate dependence of ΔM , a comparison of the

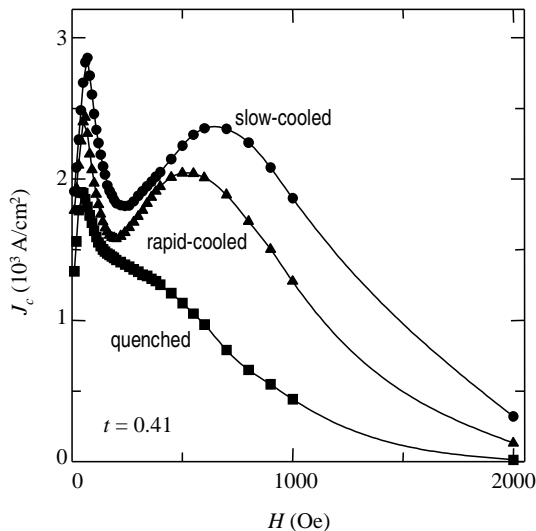


FIG. 4: Magnetic-field dependence of the critical current density at $t = 0.41$ estimated from $\Delta M(H)$ on the basis of a standard Bean's model²¹ for a square-shape sample²².

measured ΔM 's should be done at a fixed temperature t ($= T/T_c$), since cooling-rate changes T_c .

Figure 4 shows the magnetic-field dependence of the critical current density J_c at $t = 0.41$. The estimation of J_c from ΔM was carried out through a standard Bean's model²¹ for a square-shape sample²². The data at 4.5 K are used for the quenched sample, and the corresponding data at 4.7 K (rapid-cooled) and 4.9 K (slow-cooled) are calculated from a linear interpolation with the data at both 4.5 and 5.0 K, respectively. Even after the subtraction of the effect on the reduced T_c , the critical current density clearly decreases with increasing cooling-rate. This indicates the suppression of the effective vortex pinning by cooling fast. Because rapid cooling of samples is considered to induce frozen ethylene-disorders, one may expect the increase of vortex pinning. However, in the present vortex system, the effective pinning force becomes weak with increasing ethylene-disorder. This result is apparently inconsistent with a concept of the simple pinning driven by disorder.

Here we characterize the magnetic-field of the second peak. Contrary to the peak effect of $\text{Bi}_2\text{Sr}_2\text{CaCu}_2\text{O}_8$ ($\text{Bi}2212$),²³ the peak structure in the present superconductor is broad. This makes it difficult to determine a characteristic magnetic-field of the second peak without any ambiguity. We here define the peak position using two magnetic-fields: one is the magnetic-field of the minimum point between the central and second peaks (H_{\min}), and the other is the maximum point for the peak (H_p). Each magnetic-field is plotted in the T - H phase diagrams with overlaid for each cooling-process, as shown in Fig. 5. Additionally plotted irreversibility fields (H_{irr} , open

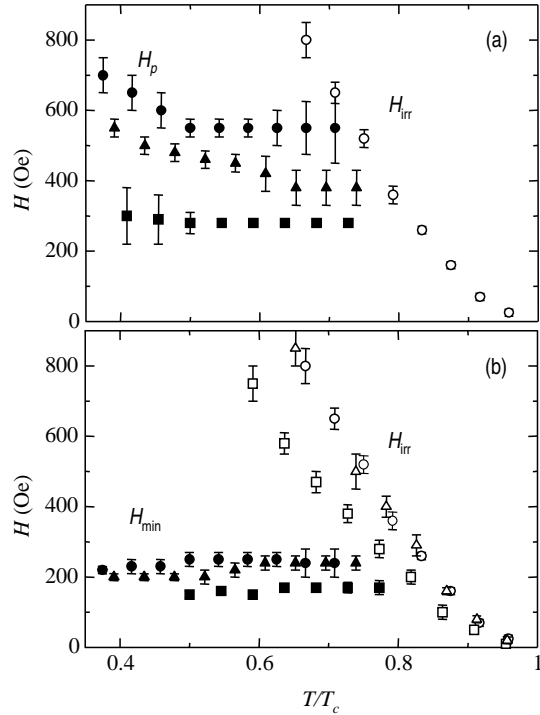


FIG. 5: Characteristic magnetic-fields (closed symbols) as a function of temperature with overlaid for the slow-cooled (circles), rapid-cooled (triangles), and quenched (squares): (a) H_p and (b) H_{\min} . H_{irr} (open symbols) is also plotted.

symbols) are defined using a criterion of $J_c = 2.0 \text{ A/cm}^2$ (corresponding to $\Delta M = 1.0 \times 10^{-5} \text{ emu}$). As a function of temperature, H_p increases with reducing temperature for all the cooling-process (Fig. 5(a)). On the contrary, H_{\min} shows the different behavior as displayed in Fig. 5(b), where the H_{\min} lines are piled around 200 Oe.

IV. DISCUSSION

We first discuss the origin of the second peak effect. The peak effect of the present compound has been attributed to the dimensional crossover of the vortex system.^{10,11,12} A vortex line changes to two-dimensional (2D) pancake vortices with the decrease of the inter-layer Josephson coupling above the crossover field $B_{\text{cr}} \approx \phi_0/(\gamma d)^2$, where ϕ_0 is the magnetic flux quantum, γ the anisotropy factor, and d the interlayer distance. With the values of $\gamma = 130 - 180$ ^{24,25} and $d = 15 \text{ \AA}$, one obtains $B_{\text{cr}} \approx 280 - 540 \text{ G}$. The estimated B_{cr} roughly corresponds to the second peak. It is almost the same as H_{\min} and H_p , and thus the dimensional crossover scenario as the second peak origin is applicable to this case. Although the broad shape of the second peak seems to be inconsistent with this interpretation, the broadness may come from the averaging of the peak structure over

the bulk sample in which the local magnetic-field has a distribution. A more detailed experimental investigation would be needed to check this point. B_{cr} is generally independent of temperature, and moreover in the present system, cooling-rate independence is expected as well, because the anisotropy factor γ is likely to be unchanged by cooling-rate. Actually, even in the deuterated BEDT-TTF based-salt, which has dramatically different electronic properties from the present (non-deuterated) salt,²⁶ the same value of γ has been reported.²⁷ While H_p decreases with increasing both temperature and cooling-rate, H_{min} is almost independent of both of them. The behavior of H_p cannot be explained by a simple dimensional crossover model. On the contrary, H_{min} seems to be appropriate as B_{cr} . If $B_{\text{cr}} \sim H_{\text{min}}$, the second peak is qualitatively explained as follows: In $H > \sim H_{\text{min}}$, two-dimensional pancakes appear, and the pinning force for the pancake vortices is effectively optimized around H_p .

Besides dimensional crossover, several models have been proposed as the origin of the second peak effect: (1) matching effects,²⁸ (2) the magnetic-field-dependent relaxation-rate (collective pinning model),²⁹ (3) the field-induced order-disorder transition (Bragg-glass to vortex-glass transition), etc. First, in (1) matching effects, the peak structure appears around a magnetic-field in which the vortex lattice structure is commensurate with the defect structure. In this model, when the number of defects increases, the magnetic-field of the peak maximum increases. However in the present case, by cooling faster which may be giving much larger number of defects, H_p shifts toward lower magnetic-fields. Thus the experimental results are inconsistent with this model. Next, the second model (2) is also excluded by the following reason; in this model, a collective pinning of vortices appears above the peak maximum field, resulting in a slower relaxation-rate than that below the magnetic-field where a single-vortex pinning mechanism governs the system. According to a relaxation measurement in the present compound¹¹, the relaxation-rate at the peak maximum field is faster than that at the peak minimum one, which contradicts with this model. The third model (3) is relatively controversial. In this model, with increasing magnetic-field, a first-order phase transition happens from a vortex lattice or Bragg glass state (ordered-solid phase) to a vortex-glass state (disordered-solid phase), lacking translational order. This transition is originated from the larger pinning energy gain of the glass phase than that of the lattice one, which can reasonably explain the peak effect. In high- T_c superconductors^{30,31}, the order-disorder transition has been observed as a steep increase or a step of magnetization, but in the present organic superconductor, there has been no decisive evidence in favor of this model. To confirm this model, it is needed to investigate, for example, the magnetization under a rapidly fluctuating magnetic-field, as has been measured in Bi2212.³¹

While the dimensional crossover explains the second peak effect, the problem of the suppressed J_c by cooling

fast is left unsettled. Note that the suppression is remarkably shown in $H > H_{\text{min}}$ (Fig. 4), in which the vortex system consists of pancakes. This implies the weakness of pinning, which will support the discussion on domain structures of the ethylene-disorders as a weak pinning origin, presented later. In the following, to understand the observed result we solve the puzzling origin of the vortex pinning.

As a pinning site, intrinsic defects such as molecular defects, dislocations, or coexist of another crystal phases are considerable. Actually a coexisting α -phase in the κ -type crystal has been observed using scanning tunneling microscopy (STM).³² However, these intrinsic defects, if any, are independent of cooling-rate. As already mentioned, our experimental results indicate that the effective pinning force is suppressed with cooling faster, that is, with increasing ethylene-disorder. Here it should be noted that the size of a BEDT-TTF molecule ($\sim 3 \text{ \AA}$ projected on the ac -plane) is much smaller than that of a vortex core ($2\xi_{\parallel}(0) \sim 50 \text{ \AA}$, where $\xi_{\parallel}(0)$ is the in-plane coherence length^{9,27}). Thus it is difficult for an *individual* ethylene-disorder to behave itself as a pinning site because of smallness of the molecular size.

We next describe the numbers of the ethylene-disorders. In the present case, the quenched condition will give the largest number of the ethylene-disorders, because the conformational disorders at room temperature are frozen by quenching. The fraction of the ethylene-disorders in the quenched condition is suggested to be about 5–20%.^{6,33} Although there are no corresponding reports after slow-cooling, we suppose that a slight number of the ethylene-disorders exist even in our slow-cooled condition. Tokumoto *et al.*⁵ reported that T_c monotonically decreases from 12.2 K to 11.7 K as the cooling-rate increases from 0.02 K/min up to 10 K/min. T_c of 11.9 K at the rate ~ 0.2 K/min in their report shows a good agreement with our slow-cooled case. Thus T_c of the present sample can furthermore increase by cooling more slowly. In other words, this result suggests that there exist some ethylene-disorders even in the present slow-cooled condition.

Next, we discuss the spatial distribution of the ethylene-disorders. At high temperatures, thermal excitation will cause a random mixing of the staggered and eclipsed molecules and/or these micro domains. The quenched process freezes a higher temperature glassy state with a random distribution of the disordered molecules. As the temperature is slowly lowered, the stable conformation (eclipsed) gradually becomes dominant. The remnant ethylene-disorders weaken the superconducting state with reducing T_c . Although the mechanism in the relaxation process of the ethylene-disorders is unclear, several relaxed states after slow-cooling are expected. The possible relaxed states are classified into following three states as shown in Fig. 6. As an example, we here assume 5% concentration of the ethylene-disorders, which will be the maximum in the slow-cooled condition.⁶ Each panel shows the molecular arrangement projected

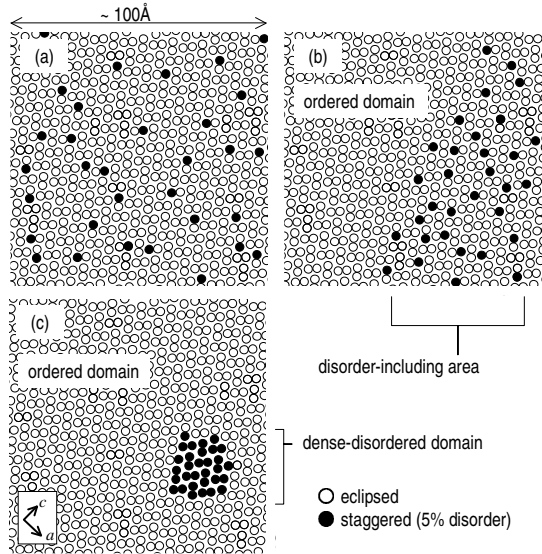


FIG. 6: Schematic views of relaxed states in the slow-cooled condition with 5% ethylene-disorders. Each panel shows the molecular arrangement projected on the ac -plane. Three possible distributions of the ethylene-disorders are described: (a) a random distributed state, (b) a state with ordered domains originated from vortex core-scale inhomogeneity, and (c) a state consisting of ordered and dense-disordered domains.

on the ac -plane over ~ 100 Å, containing about 640 BEDT-TTF and 32 disordered molecules. The BEDT-TTF molecules are described as small circles with diameter of about 3 Å, consisting of ordered (open symbols) and disordered (closed symbols) molecules. Figure 6(a) shows a state with ethylene-disorders distributed randomly, which is similar with the quenched one except for the small number of the ethylene-disorders. The second possible state shown in Fig. 6(b) features the inhomogeneous distribution of ethylene-disorders. In this case, ordered domains are formed by the increase of the stable eclipsed molecules, while remnant disorder-including areas are coexisting. A boundary structure can be formed between the ordered domain and the disorder-including area, whereas the spatial structure of the domain boundaries is unidentified. The third state is containing domains of dense-disordered molecules (Fig. 6(c)). The existence of domain structures consisting of only staggered or eclipsed molecules were suggested by the study on the relaxation of the resistivity.³⁴ Here it should be noted that the interlayer correlation of the disorder's distribution is now out of question, since we now treat the pinning of the two-dimensional pancake vortices. Therefore our description of the ethylene-disorder's distribution is also two-dimensional one, but this does not rule out the existence of the interlayer correlation of the domain structure.

Taking into account the above information on the

ethylene-disorders, we propose the domain structures of the relaxed state shown in Fig. 6(b) as a vortex pinning origin. This relaxed state contains the characteristic boundary structure between the ordered domain and the disorder-including area. The size of such a domain structure is much larger than at least the in-plane coherence length $\sim \xi_{\parallel}$ (the vortex-core-scale). In the slow-cooled condition, the widely-ordered domains dividing the disorder-including areas partly are formed, resulting in the vortex-core-scale inhomogeneity. Therefore, if these domain structures work as vortex pinning sites, the slow-cooled process gives much stronger effective pinning than the quenched one.

On the other hand, in the relaxed state shown in Fig. 6(a), many individual ethylene-disorders are distributed randomly, giving a quasi-homogeneous state on the vortex-core-scale. Therefore, the ethylene-disorders do not work as vortex pinning sites, whereas they give rise to many point defects. The quenched condition is similar with this state, while the concentration of the ethylene-disorders is much larger. Such an excess number of the ethylene-disorders may weaken the effect of the domain structure, resulting in the less effective pinning force on the vortices. This is consistent with our experimental results.

One may expect that the dense-disordered domain shown in Fig. 6(c) gives a strong pinning origin. However, the size of the domain, in spite of containing 5% ethylene-disorders, is still smaller than the vortex core. Of course one can describe a much larger dense-disordered domain structure in 5% ethylene-disorders than that of Fig. 6(c), but then the total number of the domains over the sample size becomes quite a few. So the contribution to the vortex pinning by such a dense-disordered domain cannot be so strong, if any.

An experimental support for the existence of a spatial inhomogeneity was reported by Tanatar et al³⁵, who observed a magnetic viscosity phenomena and proposed a magnetic domain structure formation in the antiferromagnetically ordered state in the normal state. Unfortunately, it is unclear whether their magnetic domain structure is directly related to the ethylene-disorders. While this may be a possible solution to the present problem, further experimental studies will be needed to check this point.

A clue might lie in a direct observation of the domain structures with local probe, such as STM, which is planning for the near future.

V. CONCLUSIONS

In conclusion, we reported the hysteretic magnetization measurements to investigate the disorder effect on the vortex pinning in the cooling-rate of 0.17, 10, and ~ 100 K/min. The negligible cooling-rate dependence of the almost full volume fraction in the superconducting state demonstrates that the superconducting volume

is unchanged by cooling-process. The second peak is observed below about 8 K for all the cooling-process. We adopt the dimensional crossover scenario as the origin of the second peak. The vortex pinning in the present system is suggested to be closely related to the ethylene-disorders. However, it is difficult for an individual ethylene-disorder to behave itself as a pinning site because of smallness of the size. Actually by cooling faster the critical current density decreases, and so the effective pinning force is apparently suppressed. Thus a simple pinning by the introduced ethylene-disorders does not occur.

To explain the puzzling pinning origin, we proposed the

ethylene-disorder domain model, where domain structures form a vortex-core-scale inhomogeneous distribution of the ethylene-disorders working as vortex pinning sites (shown in Fig. 6(b)). The size of the domain structure will be much larger than at least the in-plane coherence length. On the contrary, an excess number of disorders introduced by quenching may weaken the effect of the domain structure, which results in the less effective pinning force.

This research was partially supported by the Ministry of Education, Science, Sports and Culture, Grant-in-Aid for Encouragement of Young Scientists.

-
- ¹ T. Ishiguro, K. Yamaji and G. Saito: *Organic Superconductors*, 2nd ed. (Springer, Heidelberg, 1998).
 - ² U. Geiser, A. J. Schultz, H. H. Wang, D. M. Watkins, D. L. Stupka, J. M. Williams, J. E. Schirber, D. L. Overmyer, D. Jung, J. J. Novoa, and M. -H. Whangboo, *Physica C* **174**, 475 (1991).
 - ³ P. Wzietek, H. Mayaffre, D. Jérôme, and S. Brazovskii, *J. Phys. I France* **6**, 2011 (1996).
 - ⁴ X. Su, F. Zuo, J. A. Schlueter, M. E. Kelly, and J. M. Williams *Phys. Rev. B* **57**, R14056 (1998).
 - ⁵ M. Tokumoto, N. Kinoshita, Y. Tanaka, T. Kinoshita, and H. Anzai, *Synth. Met.* **103**, 1971 (1999).
 - ⁶ H. Akutsu, K. Saito, and M. Sorai, *Phys. Rev. B* **61**, 4346 (2000).
 - ⁷ M. A. Tanatar, T. Ishiguro, T. Kondo, and G. Saito, *Phys. Rev. B* **59**, 3841 (1999).
 - ⁸ T. F. Stalcup, J. S. Brooks, and R. C. Haddon, *Phys. Rev. B* **60**, 9309 (1999).
 - ⁹ M. Lang, F. Steglich, N. Toyota, and T. Sasaki, *Phys. Rev. B* **49**, 15227 (1994).
 - ¹⁰ F. Zuo, S. Khizroev, G. C. Alexandrakis, J. A. Schlueter, U. Geiser, and J. M. Williams, *Phys. Rev. B* **52**, R13126 (1995).
 - ¹¹ S. Khizroev, F. Zuo, G. C. Alexandrakis, J. A. Schlueter, U. Geiser, and J. M. Williams, *J. Appl. Phys.* **79**, 6586 (1996).
 - ¹² H. Taniguchi and K. Kanoda, *Synth. Met.* **103**, 1967 (1999).
 - ¹³ T. Nishizaki, T. Sasaki, T. Fukase, and N. Kobayashi, *Phys. Rev. B* **54**, R3760 (1996).
 - ¹⁴ N. Yoneyama, T. Sasaki, N. Kobayashi, M. Inada, and S. Yamada, *Synth. Met.* **120**, 815 (2001).
 - ¹⁵ T. Shibauchi, M. Sato, S. Ooi, and T. Tamegai, *Phys. Rev. B* **57**, R5622 (1998).
 - ¹⁶ L. Fruchter, A. Aburto, and C. Pham-Phu, *Phys. Rev. B* **56**, R2936 (1997).
 - ¹⁷ M. Inada, T. Sasaki, T. Nishizaki, N. Kobayashi, S. Yamada, and T. Fukase, *J. Low Temp. Phys.* **117**, 1423 (1999).
 - ¹⁸ N. Yoneyama, A. Higashihara, T. Sasaki, N. Kobayashi, and S. Yamada, *Synth. Met.* **133-134**, 223 (2003).
 - ¹⁹ M. Pinterić, S. Tomić, M. Prester, D. Drobac, and K. Maki: *Phys. Rev. B* **66**, 174521 (2002).
 - ²⁰ M. Lang, N. Toyota, T. Sasaki, and H. Sato, *Phys. Rev. B* **46**, 5822 (1992).
 - ²¹ M. Tinkham, *Introduction to Superconductivity*, 2nd ed. (McGraw-Hill, New York, 1996), p. 178.
 - ²² M. Oussena, P. A. J. de Groot, A. Marshall and J. S. Abell, *Phys. Rev. B* **49**, 1484 (1994).
 - ²³ K. Kadowaki and T. Mochiku, *Physica C* **195**, 127 (1992).
 - ²⁴ M. Pinterić, S. Tomić, M. Prester, D. Drobac, O. Milat, K. Maki, D. Schweitzer, I. Heinen, and W. Strunz, *Phys. Rev. B* **61**, 7033 (2000).
 - ²⁵ S. Kawamata, K. Okuda, T. Sasaki, and N. Toyota, *J. Low Temp. Phys.* **105**, 1721 (1996).
 - ²⁶ H. Taniguchi, A. Kawamoto, and K. Kanoda, *Phys. Rev. B* **59**, 8424 (1999).
 - ²⁷ H. Ito, M. Watanabe, Y. Nogami, T. Ishiguro, T. Komatsu, G. Saito, and N. Hosoi, *J. Phys. Soc. Jpn.* **60**, 3230 (1991).
 - ²⁸ O. Daldini, P. Martinoli, J. L. Olsoen and G. Berner: *Phys. Rev. Lett.* **32**, 218 (1974).
 - ²⁹ M. V. Feigel'man, V. B. Geshkenbein, A. I. Larkin and V. M. Vinokur, *Phys. Rev. Lett.* **63**, 2303 (1989).
 - ³⁰ T. Nishizaki, T. Naito, and N. Kobayashi, *Phys. Rev. B* **58**, 11169 (1998).
 - ³¹ N. Avraham, B. Khaykovich, Y. Myasoedov, M. Rappaport, H. Shtrikman, D. E. Feldman, T. Tamegai, P. H. Kes, M. Li, M. Konczykowski, K. van der Beek and E. Zeldov, *Nature* **411**, 451 (2001).
 - ³² H. Shigekawa, K. Miyake, H. Oigawa, Y. Nannichi, T. Mori, and Y. Saito, *Phys. Rev. B* **50**, 15427 (1994).
 - ³³ J. Müller, M. Lang, F. Steglich, J. A. Schlueter, A. M. Kini, and T. Sasaki, *Phys. Rev. B* **65**, 144521 (2002).
 - ³⁴ X. Su, F. Zuo, J. A. Schlueter, M. E. Kelly, and J. M. Williams *Solid State Commun.* **107**, 731 (1998).
 - ³⁵ M. A. Tanatar, T. Ishiguro, H. Ito, M. Kubota, and G. Saito, *Phys. Rev. B* **55**, 12529 (1997).